PROCEEDINGS A

royalsocietypublishing.org/journal/rspa

Research



Cite this article: Cherkaev A, Cherkaev E, Lurie K. 2023 Optimal structures for focusing and energy accumulation: mathematical models and intuition. *Proc. R. Soc. A* **479**: 20220342.

https://doi.org/10.1098/rspa.2022.0342

Received: 20 May 2022 Accepted: 9 August 2023

Subject Areas:

applied mathematics, differential equations, mathematical physics

Keywords:

optimal design, optimality conditions, optimal structures

Authors for correspondence:

Andrej Cherkaev e-mail: cherk@math.utah.edu Elena Cherkaev e-mail: elena@math.utah.edu

One contribution to a special feature 'Asymptotic and numerical models of acoustic, thermal and elastodynamic metamaterials' organised by Sébastien Guenneau, Agnes Maurel and Kim Pham.

THE ROYAL SOCIETY

Optimal structures for focusing and energy accumulation: mathematical models and intuition

Andrej Cherkaev¹, Elena Cherkaev² and Konstantin Lurie³

¹Department of Mathematics, and ²Department of Mathematics, University of Utah, Salt Lake City, UT, USA
³Department of Mathematics, Worcester Polytechnic Institute, Worcester, MA, USA

(i) AC, 0000-0001-7824-445X; EC, 0000-0002-5682-5453

Metamaterials and composite structures are able to manipulate waves and focus fields and currents in desirable directions. Designs based on spatial and temporal variation of material properties create structures forcing fluxes into specified parts of the domain or concentrating energy into arrays of progressively sharpening pulses. The paper discusses examples of focusing structures, mathematical and intuitive considerations that influence optimal design theory. The optimality requirement introduces zones of optimal composites with variable microgeometry. The observed absence of classical solutions motivates the extension of the class of optimal partitions to composites. Such materials also provide a solution to the problem of optimal design of a thermal lens focusing thermal fluxes when the incoming fluxes are not completely known in advance. An extension of designs to dynamical materials such as space-time checkerboard composites introduces metamaterials with additional capabilities that control the accumulation of energy in the propagating waves. The discussed mathematical methods of focusing and suitable properties alternation targeted on optimality are illustrated by physical examples.

1. Introduction

The demand for optimal structures grows with new advances in computing and production. The technologies

of micro-fabrication and three-dimensional printing may produce various structures at roughly the same price, and it is essential to know which formations are most suitable for design. Novel types of artificially engineered metamaterials and composites are the key to further technological advances, saving energy, environmental preservation with a variety of applications from imaging and energy harvesting to lightweight constructions and design of sensors and amplifiers. Theoretically investigated and experimentally verified examples of unusual properties of such materials and unexpected behaviour of the fields and stresses, include manipulating electromagnetic, acoustic and elastic fields [1,2], creating invisibility devices for electromagnetic and acoustic cloaking [3–10], composites and metamaterials with exotic properties [11–14] and design of concentrators focusing electromagnetic fields and heat fluxes [15–22]. Another type of metamaterials is dynamic composites with the properties varying not only in space but also in time [23–35]. Such spatio-temporal variability of the properties can be created with acousto-optic and magneto-optic devices [36], by four-dimensional printing [37], or by switching the material properties.

The present work discusses an approach to structural design of composites and metamaterials based on the calculus of variations. To determine the optimal design, one formulates the optimization goal (cost functional) and determines the optimal controls that might include shapes of the domains, variable material properties and optimal structures subject to given constraints. The optimal layout of materials is found by solving the corresponding variational problem. However, these problems are often non-convex, and solving them requires relaxation, i.e. appearance of composite structures optimizing the cost functional by focusing stresses, directing fluxes and currents, concentrating energy or screening objects by making them invisible. The optimality of the interfaces between materials results in their appearance as generalized or space-filling curves.

Mathematically, the discussed approach to structural optimization is rooted in the calculus of variations and control theory. The optimal control has taken its current shape in the groundbreaking works by Pontryagin *et al.* [38], and Rozonoer [39]. Soon after, Gamkrelidze [40] applied the theory of sliding regimes to optimization, i.e. he used infinitely often alternations of control values. The theory is based on the Weierstrass variation: a sharp 'triangular' perturbation of the tested trajectory. If such perturbation improves the cost, it is repeated infinitely many times; the sliding controls generate the saw-like trajectories.

Extending the sliding regimes to multi-variable systems (optimal design) is non-trivial. Physically speaking, the alternating intervals are replaced by alternating patterns, which poses a question of their optimal shapes. Eventually, it was understood that *convexification* of the Hamiltonian should be replaced by the quasi-convexification of Lagrangian [41].

Various groups of investigators worked on different aspects of these problems, doing examples and establishing bounds for effective properties along with the optimal microgeometres. Tartar & Murat [42], Murat [43] and Tartar [44] used homogenization to find optimal designs and the effective property bounds based on compensated compactness. Kohn & Strang [41] generalized the variational approaches of Morrey polyconvexity and rank-one convexity for non-convex Lagrangians and used them for developing the optimal design methodology. Bendsoe and Sigmund developed 'topology optimization' techniques for finding layouts of optimal composites in a design domain [45–47]. Allaire [48] developed and implemented a homogenization technique for optimal design. Milton, Francfort and other researchers significantly developed the theory of optimal composites [49–51]. The books [45,48,51–53] and numerous papers highlighted the development of these approaches. Optimal layouts include both original materials and their assemblies into optimal microstructures [47,54], typically with the extremal effective properties [14,55–58], and the distribution of the layouts on a macroscopic scale [45,48,52].

The present authors developed a control theory approach (the translation method) based on the earlier introduced Weierstrass-type replacement test [53,59], homogenization and *G*-convergence [60–62], and developed a multi-variable analogue of sliding regimes. The Weierstrass-type test (Lurie [53]) checks the optimality of a stationary layout of several materials

in the design domain. The following example illustrates how this test works in statics. An infinitesimal ellipse of one of available materials is inserted into the domain occupied by the other material. This inclusion results in the increment of the cost functional that depends on the eccentricity and orientation of the trial ellipse. The dependence on orientation stems from the appearance of a dipole moment due to the elliptic shape of the inclusion. Its parameters are chosen to minimize the increment generating the 'most dangerous' variation. If the desired layout is a minimizer then any increment of the functional, including the minimal (most dangerous) increment, should be non-negative; otherwise, the variation improves the cost and disproves the optimality of the tested layout. In the latter case, the layout can be improved by adding more inclusions; in the limit, it becomes a composite. The shape and orientation of the trial ellipses point to the optimal microgeometry of such a composite.

In this paper, we discuss the use of a Weierstrass-type test to analyse the structure of optimal composites and use the results for designing devices that optimally redirect and focus vector and tensor fields. In particular, such optimally structured materials provide a solution to the problem of optimal design of a thermal lens [16,52] (or heat concentrator) focusing thermal fluxes entering the domain, to a specified part of the boundary. The use of these optimally structured thermal metamaterials allows to manipulate and control the heat flux thus making heat flow in a desired direction. In the present paper, we extend the formulation of a thermal lens problem to the case of design in uncertainty [63–65] when the incoming fluxes are not completely known in advance. This is a robust optimal design problem or design for the worst-case scenario that is formulated as a minmax or maxmin optimization problem [63–67].

Another type of focusing is discussed in the context of dynamic materials (DM). The concept of dynamic composites with the properties variable in space and time was introduced by Blekhman & Lurie [24]; materials with time variable electromagnetic properties have been discussed by Morgenthaler [68]. This concept has been extrapolated to space and time-dependent variables by Lurie *et al.* [26,28,29,35,69]. The introduction to the theory of optimal DM was presented in the book [27]. This theory received further development in the papers [23,25,30–34], among others.

2. Variational problems

Consider a two-dimensional conducting domain Ω occupied by a medium of conductivity k(x). Assume for illustration that Ω is a curved rectangle sketched in figure 1a. Two opposite sides labelled Γ_2 and Γ_4 are insulated; Ω conducts current j between two other opposite sides Γ_1 and Γ_3 . The electric field is governed by the PDE

$$\nabla \cdot j = 0, \quad j = ke, \quad e = \nabla u, \quad x \in \Omega. \tag{2.1}$$

Here, u is the potential, and k is the spatially variable conductivity that takes two values: $k(x) = k_1$ in the subdomain Ω_1 , and $k(x) = k_2$ in $\Omega_2 = \Omega \setminus \Omega_1$, with $0 < k_1 < k_2 < \infty$

$$k(\chi(x)) = \chi(x)k_1 + (1 - \chi(x))k_2, \quad \chi(x) = \begin{cases} 1 & \text{if } x \in \Omega_1, \\ 0 & \text{if } x \notin \Omega_1. \end{cases}$$
 (2.2)

We consider two optimal design problems. Both ask for the interface γ between Ω_1 and Ω_2 or for layout of materials k_1 and k_2 within a given domain Ω with prescribed boundary conditions [52].

Problem A: minimal conductance. Let us fix the boundary conditions in (2.1) as follows:

$$u = 0$$
 on Γ_1 , $u = 1$ on Γ_3 , $j \cdot n = 0$ on $\Gamma_2 \cup \Gamma_4$, (2.3)

where n is the normal to the boundary. The energy is equal to the total current through Ω

$$W_A = \frac{1}{2} \int_{\mathcal{O}} k (\nabla u)^2 dx = \int_{\Gamma_2} j \cdot n ds.$$
 (2.4)

Figure 1. (a) Sketch of the domain for the problem of finding the optimal composite structure providing the minimal conductance (problem A in §2). (b, c) Optimal structures of the annulus of extremal conductance. (b) Structure minimizing the total conductance (problem A). (c) Structure minimizing the total resistance (problem B).

The optimal problem asks for the design that minimizes W_A with respect to layout $\chi(x)$. We call $C_{\min}(\Omega)$ the minimal conductance of this layout.

To avoid a trivial solution, we prescribe amounts of each material. Domain Ω is divided into two subdomains Ω_1 and Ω_2 occupied by materials k_1 and k_2 , respectively. We introduce the cost ν for the unit of less conducting material k_1 and minimize the energy plus the cost assuming that potential u satisfies boundary conditions (2.3)

$$C_{\min}(\Omega) = \min_{\chi(x)} \min_{u \in (2.3)} \int_{\Omega} \Phi(\chi, \nabla u, k(\chi), \nu) \, \mathrm{d}x \tag{2.5}$$

and

Downloaded from https://royalsocietypublishing.org/ on 26 January 2024

$$\Phi(\chi, e, k(\chi), \nu) = k(\chi)e^2 + \nu\chi, \quad e = \nabla u, \quad k(\chi) \text{ as in (2.2)}.$$

After eliminating χ that takes only two values (see (2.2)), equation (2.5) results in the non-convex variational problem for u:

$$C_{\min}(\Omega) = \min_{u \in (2.3)} \int_{\Omega} F_A(|e(x)|; k_1, k_2, \nu) \, \mathrm{d}x$$
 (2.7)

and

$$F_A(|e|; k_1, k_2, \nu) = \min\{k_1 e^2 + \nu, k_2 e^2\}, \quad e = \nabla u.$$
 (2.8)

Note that the magnitudes of optimal fields are ordered

$$|e_2(x_2)| \le |e_1(x_1)|, \quad \forall x_1 \in \Omega_1, \quad \forall x_2 \in \Omega_2,$$
 (2.9)

where e_1 and e_2 are the fields at any points of the domains Ω_1 and Ω_2 filled with materials k_1 and k_2 , respectively,

$$e_1(x) = e(x)\chi(x), \quad \forall x \in \Omega_1, e_2(x) = e(x)(1 - \chi(x)), \quad \forall x \in \Omega_2.$$

Problem B: minimal resistance. In this problem, we prescribe in (2.1) the constant normal currents on the boundary components Γ_1 and Γ_3 , assuming that the integral of these currents over the whole boundary is zero.

$$j \cdot n = 1$$
 on Γ_1 , $j \cdot n = -\alpha$ on Γ_3 , $\alpha = \frac{|\Gamma_1|}{|\Gamma_3|}$, $j \cdot n = 0$ on $\Gamma_2 \cup \Gamma_4$, (2.10)

where α is the ratio between lengths of $|\Gamma_1|$ and $|\Gamma_3|$. The boundary components Γ_2 and Γ_4 are insulated.

Downloaded from https://royalsocietypublishing.org/ on 26 January 2024

The energy W_B is expressed through the divergence-free currents j

$$W_B = \frac{1}{2} \int_{\Omega} k^{-1} (j)^2 dx = \int_{\Gamma_3} u j \cdot n \, ds, \quad \nabla \cdot j = 0.$$
 (2.11)

This energy equals the integral of the difference between the potentials on Γ_3 and Γ_1 needed to push a given current through Ω . The minimum of this energy with respect to layout $\chi(x)$ corresponds to the least resistive domain. Assuming that current j satisfies boundary conditions (2.10) and ν is the cost of the unit of more conducting material k_2 , we define the *minimal resistance* of the domain, $R_{\min}(\Omega)$, similarly to (2.5), (2.6)

$$R_{\min}(\Omega) = \min_{\chi(x)} \min_{j \in (2.10)} \int_{\Omega} \Phi(\chi, j, k^{-1}(\chi), \nu) \, \mathrm{d}x. \tag{2.12}$$

As above, elimination of χ given in (2.2) results in the optimization problem with the non-convex variational functional

$$R_{\min}(\Omega) = \min_{j \in (2.10)} \int_{\Omega} F_B(|j(x)|; k_1, k_2, \nu) \, dx, \quad \nabla \cdot j = 0$$
 (2.13)

and

$$F_B(|j|; k_1, k_2, \nu) = \min\left\{\frac{1}{k_1}j^2, \frac{1}{k_2}j^2 + \nu\right\}.$$
 (2.14)

Similar to the ordering of the fields in problem A, the magnitudes of optimal currents should be ordered:

$$|j_1(x_1)| \le |j_2(x_2)|, \quad \forall x_1 \in \Omega_1, \ \forall x_2 \in \Omega_2,$$
 (2.15)

where j_1 and j_2 are currents at any points of the domains Ω_1 and Ω_2 , respectively,

$$j_1(x) = j(x)\chi(x), \ \forall x \in \Omega_1, \quad j_2(x) = j(x)(1 - \chi(x)), \ \forall x \in \Omega_2.$$

3. Weierstrass-type variation of layout

The variational analysis formulates the requirements for optimal fields in material but does not provide a direct method for finding the optimal layout. The solution to this problem requires a combination of intuition, an educated guess, and analysis. A hint comes from the Weierstrass-type structural variation introduced in [53]. The following replacement test can check the minimality of the cost functional. Insert an infinitesimal inclusion of material k_1 into domain Ω_2 and an equal area inclusion of material k_2 into the domain Ω_1 . Choose the parameters of both inclusions to minimize the energy. If the tested configuration is optimal, no such perturbation can decrease the energy; the cost increment is always non-negative. Instead of considering the effect of two inclusions, we can check the energy increment caused by inserting one inclusion together with the material cost increase.

Optimal inclusions. Consider a region filled by material with conductivity k_0 . Assume that the current through it is due to applied potential difference at a distant boundary. Following [53], insert an infinitesimal inclusion with a different conductivity k_i and compute the energy increment; it depends on the shape of the inclusion. The variation caused by an elliptic inclusion can be computed analytically (for example, using the Eshelby formulae [70]). The increment reaches maximum if the ellipse is optimally oriented and has optimal eccentricity. For the considered problems (2.5), (2.12), the optimal ellipse degenerates into a strip oriented across or along the current.

Increment of the functional. Consider an infinitesimal strip of material k_i inserted in a domain occupied by the host material k_0 . Let \mathbf{n} and \mathbf{t} be, respectively, the normal and tangent to the boundary of the strip, and let ω be the area of the strip. The inserted and replaced materials costs are $v_i\omega$ and $v_0\omega$, respectively.

Present the vector field $e = \nabla u$ at a point outside the strip infinitesimally close to the strip boundary in the (\mathbf{n}, \mathbf{t}) coordinates as $e = e_n \cos \theta \, \mathbf{n} + e_t \sin \theta \, \mathbf{t}$. The continuity conditions at the strip boundary require continuity of the tangent component of ∇u , $e_t = \nabla u \cdot \mathbf{t}$, and continuity of the normal component of the current $j \cdot \mathbf{n} = k \, e_n$. In the (\mathbf{n}, \mathbf{t}) coordinates, the field e_i inside the strip is

$$e_i = e_{in} \cos \theta \, \mathbf{n} + e_{it} \sin \theta \, \mathbf{t}, \quad e_{it} = e_t, \quad e_{in} = \frac{k_0}{k_i} e_n.$$
 (3.1)

The energy density W_0 outside the strip is

$$W_0 = k_0 |e|^2 = k_0 (e_t^2 + e_n^2),$$

and the energy density W_i inside the strip is

$$W_i = k_i(e_{it}^2 + e_{in}^2) = k_i e_t^2 + \frac{k_0^2}{k_i} e_n^2.$$

The increment ΔW of the energy caused by the inclusion is

$$\Delta W_{i0} = W_i - W_0 = \left[(k_i - k_0)(e_t)^2 + k_0 \left(\frac{k_0}{k_i} - 1 \right) (e_n)^2 \right] \omega, \tag{3.2}$$

and the increment in the materials' cost is $(v_i - v_0)\omega$.

Downloaded from https://royalsocietypublishing.org/ on 26 January 2024

Observe that the energy increment (3.2) depends on the orientation of the strip θ . In problem A, the maximum of ΔW_{i0} with respect to θ is reached when $\theta = 0$, or when the strips are oriented so that the normal \mathbf{n} to the strip is parallel to the electric field: $\mathbf{n} \parallel e$ and $e_n^2 = |e|^2$.

$$\Delta W_{i0}^{\text{max}} = k_0 \left(\frac{k_0}{k_i} - 1 \right) |e|^2 \omega.$$

We perform two variations placing the strip from material k_1 into the domain Ω_2 and vice versa, keeping the areas of the strips equal; the total increment is independent of the materials costs. The increment is

$$W_{12} + W_{21} = \frac{k_2 - k_1}{k_1 k_2} [(|j_1|)^2 - (|j_2|)^2] \omega,$$

where j_1 and j_2 are the currents at some points of the domains Ω_1 and Ω_2 , respectively. The increment is non-negative, $W_{12} + W_{21} \ge 0$, if the magnitudes of currents j = ke in the optimal domains are ordered together with the magnitudes of fields e, see (2.9).

Problem B can be reduced to the problem A by using $1/k_1$ and $1/k_2$ instead of k_1 and k_2 , respectively, and rotating the vector fields by 90° . The 90° rotated field e becomes the div-free current j. For isotropic materials, the energy keeps its form, but the materials are inversely ordered; the optimal strip is 90° rotated.

Physical explanation of the optimal orientation of strips. The physical explanation of the optimal orientation of the strips is as follows. In problem A, we insert a bad conductor $k_1 < k_2$ in the domain Ω_2 of the good conductor k_2 to decrease the total conductance. The maximal increment of the cost functional requires a strip placed perpendicular to the current's direction; the strip works as a barrier. A thin strip of good conductor k_2 placed perpendicular to the current in Ω_1 minimally increases the conductivity.

In problem B, the optimal inclusion of a good conductor $k_2 > k_1$ in the domain Ω_1 should maximally decrease the total resistance. The maximal increment corresponds to a strip placed along the current j; the inclusion works as a channel (wire). The orientation of optimal inclusions suggests that the interface should be oriented along the current. The strip from the bad conductor hides in the domain of a good one itself if it is oriented along the current.

Convexity. The Lagrangian F_A is a non-convex function of |e|, see (2.8). The Weierstrass test shows that for an optimal design, the current magnitude $j = \partial F_A/\partial |e|$ increases as a function of |e| or the Lagrangian is convex at the solution of the variational problem. This feature implies that argument |e| never takes values in the interval of non-convexity of $F_A(|e|)$. In this *forbidden interval* (z_-, z_+) of ∇u , neither material is optimal. The field $e = \nabla u$ in an optimal solution should avoid the forbidden interval, $|e| \notin (z_-, z_+)$, where

$$z_{-} = \sqrt{\frac{k_{1}}{k_{2}}} v^{*}, \quad z_{+} = \sqrt{\frac{k_{2}}{k_{1}}} v^{*} \quad \text{and} \quad v^{*} = \sqrt{\frac{v}{k_{2} - k_{1}}}.$$
 (3.3)

At endpoints z_-, z_+ of this interval, the tangents |j| to $F_A(|e|)$ are identical.

The minimum of energy requires that if $|e| \le z_-$, then $k = k_2$, and if $|e| \ge z_+$, then $k = k_1$. In the intervals of convexity of F_A , |j| is a monotonic function of |e|, and at the ends of the forbidden interval of non-convexity, the current densities $|j_1| = k_1 z_+$ and $|j_2| = k_2 z_-$ are equal, $j_1 = j_2$.

An optimal layout must be organized so that the density |e| jumps over the forbidden interval at the interface γ between Ω_1 and Ω_2

$$\frac{|e|_{\Omega_1}}{|e|_{\Omega_2}} = \frac{k_2}{k_1} \quad \text{on } \gamma.$$

On the other hand, the compatibility condition requires that the tangent derivative of e is continuous, and the jump of the normal derivative equals

$$\frac{e \cdot n|_{\Omega_1}}{e \cdot n|_{\Omega_2}} = \frac{k_2}{k_1} \quad \text{on } \gamma,$$

where n is normal to the interface. Comparing these conditions, we find that the interface γ must be oriented so that $|e| = e \cdot n$, hence the interface is perpendicular to vector $e = \nabla u$. The optimal interface coincides with the level lines u = constant. It remains to investigate whether or not such an interface exists: our analysis tacitly assumes that the interface line is differentiable and has a normal almost everywhere.

4. Optimal structures

Optimal structures in problem A. The composite structures that are stable against the Weierstrass-type strip variations are optimally oriented laminates (across the current), and their volume fractions m_1 and m_2 of materials are optimally chosen. Adding an optimal inclusion—a tiny strip codirected with the laminate changes only its local volume fraction. Since the fraction in the tested laminate structure is assumed to be optimal, such variation does not improve the cost. The effective conductivities of the laminates k_h and k_a across and along the layers are, respectively, harmonic and arithmetic means:

$$k_h = \left(\frac{m_1}{k_1} + \frac{m_2}{k_2}\right)^{-1}, \quad k_a = m_1 k_1 + m_2 k_2, \quad m_2 = 1 - m_1.$$
 (4.1)

According to Reuss–Voigt bounds, the eigenvalues κ_1 and κ_2 of conductivity tensor K_* of any mixture of materials k_1, k_2 in proportions m_1 and m_2 lie between harmonic k_h and arithmetic k_a

Downloaded from https://royalsocietypublishing.org/ on 26 January 2024

$$k_h \le \kappa_1, \kappa_2 \le k_a. \tag{4.2}$$

We enlarge the set of design materials, adding to the given two materials k_1 and k_2 all optimally oriented laminates of them and end up with the *relaxed* Lagrangian

$$W_{AR} = \min_{m_1 \in [0,1]} [k_h(m_1)e^2 + \nu m_1]. \tag{4.3}$$

The optimality condition

$$\frac{\partial W_{AR}}{\partial m_1} = \frac{k_2 - k_1}{k_1 k_2} |k_h e|^2 + \nu = 0, \quad \text{if } m_1 \in (0, 1),$$

shows that the current density $|j| = |k_h e|$ in the composite zone is constant.

We have demonstrated that the Weierstrass test reveals the deficiency of the solution of a variational problem; it also suggests a way to relax the problem. If a problem does not satisfy the Weierstrass-type test, one can introduce the minimal extension of Lagrangian by including fast oscillating optimally oriented strips into the set of admissible layouts. The procedure is similar to convexification of a non-convex Lagrangian.

Optimal structures in minimal resistance problem (problem B). In this problem, the function $F_B(j)$ (2.14) is algebraically similar to $F_A(e)$ in (2.8). There is a forbidden interval $j \in (j_-, j_+)$ of non-convexity for the |j| values. The graph of $F_B(|j|)$ has a common tangent at these points, similarly to (3.3)

$$\frac{|j|_{\Omega_1}}{|j|_{\Omega_2}} = \frac{k_1}{k_2}. (4.4)$$

If the value of |j| is below the forbidden interval, $|j| \le j_1$, then $k = k_1$; if $|j| \ge j_+$, then $k = k_2$ (compare with (3.3)). Similarly to problem A, at the end of the forbidden interval, $|e| = \partial W_B/\partial |j|$ takes equal values.

On the other hand, the compatibility condition at the interface between Ω_1 and Ω_2 requires the jump of the tangent τ derivative

$$\frac{j \cdot \tau|_{\Omega_1}}{j \cdot \tau|_{\Omega_2}} = \frac{k_1}{k_2}.\tag{4.5}$$

Referring to the forbidden interval, we conclude that the tangent τ to the interface must be collinear with j; the optimal interface coincides with a streamline. The optimal composite structures are laminates oriented along the current.

(a) Example: axisymmetric design

Consider a plane annulus Ω , $r_0 \le r \le 1$, $-\pi \le \theta < \pi$, and assume that the constant potentials are applied at its inner and outer circular boundaries [52]. It is required to distribute two materials with conductivities $k_1 < k_2$ taken in a fixed overall proportion within Ω to maximize or minimize its integral conductance. Because of axial symmetry, the current j flows radially and depends on r only, j = j(r); its density decreases inversely proportional to the radius, $j(r) = j_0/r$.

Problem A. Place materials in Ω to minimize the total conductance. The optimality requires placing k_1 where the current density is maximal, that is near the inner radius, $r \in [r_0, r_1]$, where r_1 is the radius of material interface. The material k_2 will occupy the outer annulus $r \in (r_1, 1]$. Indeed, the current lines are directed along the radii. We have seen in (4.4), (4.5) that an optimal infinitesimal inclusion is a strip perpendicular to the current direction, i.e. along with the concentric circles. Accordingly, the interface between Ω_1 and Ω_2 is perpendicular to the current's direction and is a circle $r = r_1$. We check that the current is continuous at this interface. The worst conductor is placed inside, the best one—outside.

Problem B. Place materials in Ω to minimize the total resistance (to maximize the total conductance). The optimality requires placing k_2 where the current density is maximal, that is, near the inner annulus, while the material k_1 occupies an outer annulus. The question is how to find the interface between them. The optimal interface γ between the subdomains should be parallel to the current lines, i.e. along the radii. This interface can be approximated by a zigzag 'sawlike' curve oscillating between the inner and outer boundaries. The approximation is better when the zigzags are denser because the oscillating interface is closer to radii. In the limit, γ turns into a generalized curve that densely covers an annulus $r_a \le r \le r_b$. Physically speaking, we come to a composite that occupies a region $r_a \le r \le r_b$; the proportion m_1 of k_1 varies in the laminates from zero at the inner radius $r = r_a$ to one at the outer radius $r = r_b$. This laminate consists of radial 'wires' that conduct the current from the centre to the periphery. No parameter restricts the thickness of the wires; they are infinitely thin, and their number is infinitely large. The behaviour of such a composite is described in homogenized terms.

Let us determine the optimal parameters of the laminate. The current density $j(r) = j_0/r$ in composite decreases inversely proportional to the radius; the current densities j_1 and j_2 in each material stay constant at the boundaries of the forbidden interval; the total current j(r) varies with the volume fraction m_1 of k_1 , $j(r) = m_1j_1 + (1 - m_1)j_2$; this fraction depends on r and increases from zero to one

$$m_1(r) = \frac{j_0/r - j_2}{j_1 - j_2}.$$

The last feature physically means that layers from k_1 of very low density enter the region occupied by material k_2 at the radius $r = r_a$, forming thin radial bridges. The bridges' density grows with the radius, and at $r = r_b$, they fill the entire domain, which becomes the region of the material k_1 .

Note that: (i) the current density in each material is constant in the composite zone, (ii) the laminates that support this constancy are composed of infinitesimally fine layers, and (iii) the average current varies only due to slow changes of $m_1(r)$. These features are typical for optimal designs.

Smooth boundaries and generalized laminate boundaries. One may wonder why the composite appears in problem B but does not in problem A. Problem A is exceptional because its axial symmetry automatically provides orthogonality of the gradient to the material interfaces. If the domains are not symmetric, the lamination appears in both solutions. Optimal structures of the annulus of minimal conductance and minimal resistance are shown in figure 1*b*,*c*.

(b) Variational problem for multiple potentials

Consider a conducting rectangular plate $\Omega: a \times b, a < b$. It is assembled from two materials taken in a prescribed proportion. Assume that two independent experiments are conducted. In each of them, the propagating current is due to different boundary potentials, the a sides and b sides of Ω . The optimization problem asks to minimize the total conductance of the domain, that is the sum of current energies, see [44,58].

Proceeding as before, we examine the shape and orientation of the most sensitive Eshelby inclusion. The results [52] are as follows: the shape of the ellipse filled with a better conductor (k_2) depends on the relative intensities of orthogonal currents. It does not always degenerate into a strip. If the intensities are equal, the optimal shape is a circle. In general, the optimal shape is either an ellipse with eccentricity dependent on the ratio of local currents, or a strip if this ratio is larger than a threshold. The inclusion 'hides' itself in the surrounding material to minimize its effect on conductance. On the contrary, the worst conducting inclusion from k_1 always degenerates into a strip oriented across the larger current. It 'displays' itself to minimize the conductance. The collection of such inclusions forms a composite with the inclusions of conductivity k_2 in the matrix of material k_1 . This composite has a variable degree of anisotropy and volume fraction of inclusions; it may degenerate into a laminate if one of the applied currents is much larger than the other.

This structure is an example of a second-rank laminar optimal structure or a laminate made from laminates, see figure 3. It is shown in [58] that a second-rank laminate has extremal conductivity in a chosen direction, assuming the conductivity in an orthogonal direction is given. The optimal degree of anisotropy depends on the ratio of applied currents. Later this concept was further developed in many works, see for example, [11,14].

The effective (homogenized) anisotropic conductivity K_{l2} of second-rank laminates satisfies the relations [44,58,71]

$$\operatorname{Tr}(K_{l2} - k_2 I)^{-1} = m_1 \left(\frac{2}{k_1 - k_2} + \frac{m_2}{2k_2} N \right), \quad K_{l2} - k_2 I \ge 0, \tag{4.6}$$

where I is a unit matrix, and N is a non-negatively defined matrix with unit trace, Tr N = 1; the matrix N determines the degree of anisotropy.

The geometry of optimal composites is not unique. Several other equivalent microstructures are known to be optimal. Examples of such structures are the Hashin–Shtrikman coated circles [72], and, for anisotropic loading, coated ellipses [73] and other structures [51,73]. They have the same effective conductivity as the second-rank laminates. More complex problems require more advanced optimal structures, some examples of them are shown in [12,14,51,56,74].

5. Structural optimization

Downloaded from https://royalsocietypublishing.org/ on 26 January 2024

(a) Constrained variational problem

Consider optimal design of a conducting body [52,53]. It is required to minimize a functional of the type

$$P = \min_{k(x)} \int_{\Omega} G(u, \nabla u) \, \mathrm{d}x + \int_{\Gamma} g(u, u_n) \, \mathrm{d}s; \quad u_n = \frac{\partial u}{\partial n}, \tag{5.1}$$

where n is the normal to Γ , k is as in (2.2) and u is the potential in the boundary value problem

$$\nabla \cdot q = 0$$
, $q = k(x)\nabla u$ in Ω , $\Psi(u, u_n) = 0$ on Γ , (5.2)

where q is an electric current, k is a varying conductivity of material in the domain Ω .

Equation (5.2) is a differential constraint on potential u. We account for this constraint by adding it to the functional with the Lagrange multiplier $\lambda = \lambda(x)$, which is a solution of the adjoint boundary value problem

$$\nabla \cdot \left[k(x) \nabla \lambda + \frac{\partial G}{\partial (\nabla u)} \right] - \frac{\partial G}{\partial u} = 0 \quad \text{in } \Omega, \quad \lambda + \frac{\partial g}{\partial u} - \lambda_n - \frac{\partial g}{\partial u_n} = 0 \quad \text{on } \Gamma.$$
 (5.3)

Assuming that (5.2) and (5.3) are satisfied, and the optimal layout of materials in the domain might be provided by the microstructure of a possibly anisotropic composite with the effective tensor K_* , we arrive at the cost P defined as the value of the minimax functional

$$P = \min_{K_*(x)} I(K_*, \lambda, u), \quad I(K_*) = \min_{u} \max_{\lambda} \int_{\Omega} \nabla \lambda \cdot K_* \nabla u \, dx.$$
 (5.4)

The problem (5.4) introduces a locally optimal tensor K_* as a function of $\nabla \lambda$ and ∇u .

Weierstrass-type test. The structural Weierstrass test [53] consisting of insertion of inclusion in domain occupied by an isotropic material, also hints for an optimal structural design. We assume that the values of ∇u and $\nabla \lambda$ are fixed, and minimize the increment of integral in (5.4) caused by this inclusion. The result of this test shows that (a) optimal inclusion is a strip, and (b) it is oriented along the bisector of the angle between ∇u and $\nabla \lambda$. The test suggests that optimal design includes laminates and hints on their orientation.

It has been shown in [53] that the Weierstrass test leads to contradiction in the original formulation: the optimal orientation of the trial strip shows the normal to the interface, whereas the orientation of the interface is defined by an independent Weierstrass–Erdmann condition.

Generally, these two conditions contradict each other and make the problem overdetermined. The inconsistency arises because the critical orientation of a trial strip is dictated by the requirement of optimality. It may be overcome if the class of admissible materials is extended to include all anisotropic composites assembled from the original constituents (see more details below).

(b) Example: coil

This example [52] demonstrates the optimal design with some counterintuitive features. Consider a conducting thin hollow cylinder Ω of unit height z=1 and unit radius; its surface in cylindrical coordinates z,θ is: $\Omega=[0,1]\times[-\pi,\pi]$. Assume that the potentials at the bottom and top of the cylinder are equal to zero and one, respectively: $u(0,\theta)=0$, $u(1,\theta)=1$. The surface is assembled from two conductors; their amounts are not prescribed. The problem is to maximize the surface integral of the circumferential component $j_{\theta}=J\cdot \mathbf{i}_{\theta}$ of the current, that is the component perpendicular to the potential gradient, $\nabla u=\mathbf{i}_z$.

We put $G(u, \nabla u) = -\nabla u \cdot \mathbf{i}_{\theta}$ and $g(u, u_n) = 0$ in (5.1). The boundary value problem for λ becomes

$$\nabla \cdot K_*(x)\nabla(\lambda + \mathbf{i}_{\theta}) = 0 \text{ in } \Omega, \quad \lambda_n = 0 \text{ on } z = 0, 1.$$

It has a constant solution $\nabla \lambda = -\mathbf{i}_{\theta}$.

A pure material is not optimal because j_{θ} is zero on a homogeneous cylindrical surface: the current flows along the cylinder's rulings. The optimal design is a composite. It is clear that (i) the conductivity tensor K_* of an optimal composite is constant in Ω , and (ii) the most anisotropic composite is optimal. Such composite is a laminate. It directs the current to maximal possible degree because its effective conductivities k_h and k_a are extremal, see (4.2). Optimal tensor K_L of laminate conductivities depends on the volume fraction m_1 of material k_1 and the orientation ϕ of its eigenvectors (the angle between the laminate and the cylinder's rulings), $K_L = K_L(m_1, \phi)$. It remains to calculate these parameters from (5.4). Since the integrand is constant, the problem becomes algebraic

$$\min_{m_1,\phi} \mathbf{i}_{\theta} \cdot K_L(m_1,\phi) \mathbf{i}_z.$$

The calculation shows that one of the eigenvectors bisects the angle between i_{θ} and i_{z} . The optimal layers are directed at 45° to the rulings. The direction corresponds to the optimal orientation of the trial strip in the Weierstass test. The optimal volume fraction is computed as

$$m_{\text{opt}} = \frac{\sqrt{k_1}}{\sqrt{k_1} + \sqrt{k_2}}.$$

The optimal structure that most effectively rotates the current is a coil.

Thermal lens. Usually, the heat dissipates in materials. The optimal design can resist dissipation by making a 'thermal lens' [16], which focuses heat flux into a specified region. Figure 2b shows an example of an optimal focusing thermal lens. Consider a plane rectangular domain $\Omega: [-a,a] \times [0,1]$, see figure 2a. The domain is divided into two parts $\Omega = \Omega_1 \cup \Omega_2$ occupied, respectively, by two conductors of conductivity $k = k_1$ and $k = k_2$, $0 < k_1 < k_2$. Assume that unit heat flux $q = -k \nabla u$ enters Ω across its top boundary Γ_1 , the lateral sides Γ_2 and Γ_4 are insulated, and constant temperature u = 0 is maintained along the bottom boundary Γ_3 . The temperature field u = u(x) in Ω is governed by equations (5.2)

$$\nabla \cdot q = 0, \quad q = -k \nabla u, \quad k = k_1 \chi(x) + k_2 (1 - \chi(x)) \text{ in } \Omega$$
 (5.5)

and

$$n \cdot q|_{\Gamma_1} = -1, \quad n \cdot q|_{\Gamma_2 \cup \Gamma_4} = 0, \ u|_{\Gamma_3} = 0,$$
 (5.6)

where n is the outer normal. We are interested in finding an arrangement of materials in the domain Ω (or finding the regions Ω_1 and Ω_2) that maximizes the heat flux through the window

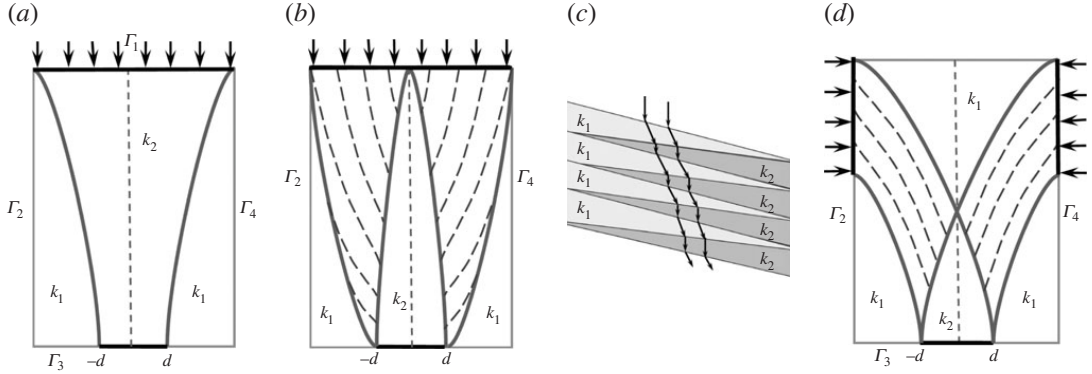


Figure 2. (a) Funnel-type (intuitively) rational layout of materials k_1 and k_2 in thermal lens directing heat from the top surface Γ_1 to the window [-d,d] at the bottom part of the boundary Γ_3 . This design is not optimal. (b) A sketch of the optimal thermal lens design with zones of pure isotropic materials k_1 and k_2 and anisotropic composite zones. (c) Cartoon of the composite zone between the regions filled with materials k_1 and k_2 with the black broken lines showing the direction of the heat flux in each of the materials. The slopes of these lines change at each interface, directing the heat flux into the desired region. (d) A sketch of the robust design of optimal thermal lens with zones of pure isotropic materials k_1 and k_2 and anisotropic composite zones forcing the heat to flux in the desired direction. The robust design maximizes the heat flux out of the window [-d,d] located at Γ_3 for any of the fluxes (not known in advance) through the parts of the boundary Γ_2 or Γ_4 at the opposite sides of the domain Ω .

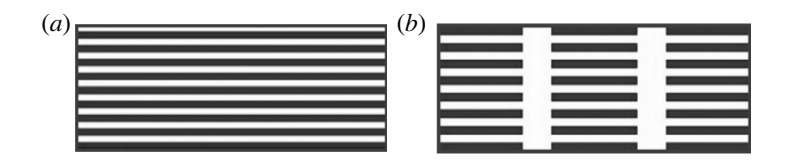


Figure 3. (*a* and *b*) First-rank and second-rank laminates used in optimal minimax design.

 $|x| \le d$ on Γ_3

$$I = \max_{\chi} j, \quad j = \int_{\Gamma_3} \rho \, q \cdot n \, dx, \quad \rho(x) = \begin{cases} 1, & |x| \le d, \\ 0, & d < |x| < a, \end{cases}$$
 (5.7)

where *q* satisfies (5.5), (5.6). This problem becomes the one described in §a if we put G = 0, $g = \rho q \cdot n|_{\Gamma_3}$.

Analysis. Referring to the previous examples, see §4c, we assume that the optimal layout includes a binary composite characterized by an effective conductivity tensor K_* with the eigenvalues satisfying the Reuss–Foigt bounds (4.2). The system of optimality conditions consists of equations (5.5) and (5.6), equations for the adjoint function λ ,

$$\nabla \cdot K_* \nabla \lambda = 0 \quad \text{in } \Omega \tag{5.8}$$

and

$$n \cdot K_* \nabla \lambda = 0 \text{ on } \Gamma_1, \Gamma_2, \Gamma_4, \quad \lambda = \rho \text{ on } \Gamma_3,$$
 (5.9)

and for the optimal effective tensor K_{opt}

$$K_{\text{opt}} = \arg\max_{K_*} (\nabla \lambda)^T K_* \, \nabla u. \tag{5.10}$$

Note that the adjoint variable differs from zero, $\lambda \neq 0$, due to the boundary condition $\lambda = \rho$ on Γ_3 ; in other words, it accounts for the cost functional, see (5.7).

Finally, we find an optimal value of volume fraction m_1 in the laminate. Call 2ϕ the angle between $\nabla \lambda$ and ∇u and rewrite (5.10)

$$K_{\text{opt}} = \arg \max_{K_L} (\nabla \lambda)^T K_L \, \nabla u = |\nabla \lambda| \, |\nabla u| \, \max_{m_1} (-k_h(m_1) \sin^2 \phi + k_a(m_1) \cos^2 \phi). \tag{5.11}$$

The volume fraction m_{opt} of m_1 in K_{opt} depends on the angle between $\nabla \lambda$ and ∇u but does not depend on their magnitudes. We have

$$m_{\text{opt}} = \begin{cases} 0 & \text{if } \tan \phi \le \sqrt{\frac{k_1}{k_2}}, \\ \frac{\sqrt{k_1 k_2}}{k_2 - k_1} \left(\tan \phi - \sqrt{\frac{k_1}{k_2}} \right) & \text{if } \tan \phi \in \left[\sqrt{\frac{k_1}{k_2}}, \sqrt{\frac{k_2}{k_1}} \right], \\ 1 & \text{if } \tan \phi \ge \sqrt{\frac{k_2}{k_1}}. \end{cases}$$
(5.12)

The optimal laminate becomes an isotropic material with maximal conductivity k_2 when the directions of $\nabla \lambda$ (what we want) and ∇u (what we have) are close to each other, it becomes an isotropic material with minimal conductivity k_1 if those directions are close to opposite. The conductivity is anisotropic when $\nabla \lambda$ and ∇u are close to orthogonal. The thermal lens focuses the flux into the target region and expels it from unwanted domain. In the region in between, it guides the flux in the desired direction due to its refraction in the anisotropic laminates.

Downloaded from https://royalsocietypublishing.org/ on 26 January 2024

Remarks about the optimal design of thermal lens. An intuitive draft of the focusing device is sketched in figure 2a. However, from the analysis presented in the previous part, the optimal design of thermal lens should have composite zones. The optimal distribution of materials in the domain Ω is shown in figure 2b. A similar conclusion can be derived using the Weierstrass-type variation. By optimizing parameters of a trial ellipse [53], one finds that it (a) degenerates into a strip, and (b) this strip is oriented along the bisector of the angle between ∇u and $\nabla \lambda$ [16,52]. These two features suggest that the optimal composite is a laminate, and the layers are oriented along the optimal trial strip.

The optimal thermolens combines the features of the already discussed designs. Similar to the axisymmetric domain of minimal resistance, it is a laminate with volume fractions varying along the layers. At the opposite boundaries of the composite zone where $m \to 1$ or $m \to 0$ the effective conductivity coincides with the conductivity k_1 or k_2 , respectively; the effective conductivity is continuous everywhere. Similarly to the coil design, the anisotropic laminates affect the direction of the flux; they work as a focusing instrument. To better understand this effect, examine a magnified element of the laminate shown in figure 2c. Consider a bundle of vector lines of the heat flux passing through a magnified piece of laminate. There are discontinuities (kinks) of the slope of those lines as they intersect the material interfaces; in the limit, there are infinitely many kinks. Each one contributes to the final orientation of vector lines targeted towards the window.

There is another (heuristic) argument in favour of zigzag (composite) material geometry in a transitional zone separating original isotropic materials k_1 and k_2 . This argument is based on an assumption of the existence of a smooth differentiable curve between the pure materials and a demonstration that this leads to a contradiction [53]. Indeed, analysis of the Weierstrass–Erdmann conditions and the most 'dangerous' orientation of the trial inclusion located close to the boundary, shows that the boundary should frequently oscillate between the areas occupied by pure materials (figure 2c). This contradiction can be avoided by introducing a space-filling curve

as the transition boundary instead of a simple curve. The microstructure may occupy a domain in the (x, y)-plane, in which case it requires homogenization.

In both cases, the Weierstrass-type variation suggests an extension of the set of admissible designs by creating an anisotropic composite controlling the direction and intensity of the heat flux. In optimal design, the interface Γ becomes a space-filling curve that densely covers a part of Ω . This region is occupied by laminated composite assembled from original materials, figure 2c. The varying volume fractions of materials and orientation of the layers represent controls.

6. Minimax robust design

Let us return to the problem of extremal conductance and assume that constant potentials $u_0 = 0$ and $u_1 = 1$ are applied to opposite boundaries of a rectangular domain Ω ; the other boundaries are insulated. Assume also that *a priori* we do not know whether the potentials are applied to vertical or horizontal sides, *a* and *b*, respectively.

The problem is to minimize the effective conductivity of the domain. To deal with this uncertainty in the boundary conditions, we reformulate the problem as optimization in a worst-case scenario—as the problem of minimization of the maximal of two effective conductivities.

Following described principles, we assume that the rectangle is filled with a homogeneous anisotropic composite with effective tensor K_{l2} in (4.6). Let its principal conductivities (eigenvalues of K_{l2}) be κ_1 and κ_2 . According to Reuss–Voigt inequalities (4.2), κ_1 and κ_2 are bounded by the eigenvalues κ_a and κ_h of the laminated composite, in the directions along and across the electric field, respectively. As we are interested in the minimal and maximal conductivities, we can assume that the eigenvectors of K_{l2} are oriented along the sides of the rectangular domain Ω . If the potential difference is applied between the sides a, then laminated composite oriented along a has the minimal conductivity k_h , and the conductance C_a of the rectangle is

$$C_a = \frac{b}{a} k_h.$$

When the potential difference is applied between the sides b, the conductance of that laminated rectangle C_b is

$$C_b = \frac{a}{b} k_a,$$

because the conductivity of laminate is $k_a > k_h$. If $C_a \le C_b$, that is

$$\frac{a^2}{b^2} \le \frac{k_h}{k_a},$$

then the optimal composite is a simple (first-rank) laminate, figure 3a. The conductance of C_a is still larger than C_b and the conductivity along the current line is the minimal possible.

If $C_a \ge C_b$, then an optimal solution corresponds to equal conductivities in both cases. The optimal composite, figure 3b, is a second-rank laminate (4.6) with the eigenvalues satisfying the additional relation

$$\frac{a}{b}\kappa_1 = \frac{b}{a}\kappa_2.$$

The optimal designs are shown in figure 3.

Robust design of thermal lens. The discussed optimal structures are designed to conduct and direct given boundary flux q. Their performance is no longer optimal if this flux is applied at a different part of the boundary. In various applications, it is of interest to design a robust project that works well for several boundary fluxes q_1, \ldots, q_n imposed on the boundary of the domain. A robust max-min design problem determines a layout K_* that maximizes the cost $I(q, K_*)$ for the

$$I = \max_{K_* \in \mathcal{GK}} \min_{k=1,..,n} I(q_k, K_*).$$

Here, \mathcal{GK} is the set of effective properties of all composites assembled from materials with properties k_1 and k_2 . This set is called *G-closure* of $\{k_1, k_2\}$, see [54,58]. The problem of robust optimal design (or optimal design in uncertainty) was formulated in elasticity setting in [63] and further studied in [64,65,75].

To illustrate the approach to robust design using the thermal lens example, we assume that the boundary fluxes are only partially known. Specifically, we assume that the heat flux may enter either through the boundary component Γ_a located on lateral side Γ_2 or through Γ_b located on the opposite lateral side Γ_4 (figure 2d). The lower boundary Γ_3 is kept at zero temperature, and the rest of the boundary $\Gamma_{\rm ins}$ is insulated. The design aims to maximize the flux through the window Γ_0 located at Γ_3 , for the most undesirable choice of the applied fluxes. The design should provide the channelling of the heat toward the window, but the heat flux could be caused by one of two fluxes (not known in advance) entering at the opposite sides of Ω .

Let K_* be the tensor of the effective conductivity and $I_a(K_*)$ and $I_b(K_*)$ be the total fluxes through the window Γ_0 corresponding to the fluxes at Γ_a and Γ_b , respectively. The optimization problem is formulated as

$$I = \max_{K_*} \min\{I_a(K_*), I_b(K_*)\}.$$

The boundary value problems for the temperature distributions u_a and u_b in the two described cases of loading are, respectively

$$\nabla \cdot q = 0$$
 in Ω , $q = -k \nabla u$, $q \cdot n|_{\Gamma_{\text{ins}}} = 0$, $u|_{\Gamma_3} = 0$, (6.1)

with different conditions in the cases (a) and (b) on the parts of the boundary Γ_a , Γ_b

(a)
$$q \cdot n|_{\Gamma_a} = 1$$
, $q \cdot n|_{\Gamma_b} = 0$, (b) $q \cdot n|_{\Gamma_a} = 0$, $q \cdot n|_{\Gamma_b} = 1$. (6.2)

We are looking for the layout $K_{\text{opt}}(x)$ that maximizes the integral of the smallest of the fluxes through the window on the lower side of Ω , see the problem (5.7),

$$I = \max_{K_*} \min\{I_a, I_b\}$$
 and $I_{a,b} = \int_{\Gamma_3} \rho \, q_{a,b} \cdot n \, dx.$ (6.3)

Here, the symbols $()_{a,b}$ refer to the corresponding problem for u_a and u_b in (6.1)–(6.2), respectively.

What structure is optimal in this robust problem? The minimum of the energy of the domain corresponding to one of the two different heat sources is provided by second-rank laminates (inclusions of the bad conductor into the good conductor) that conducts heat well in both directions. Surprisingly, the optimal layout in the current problem is a simple (first-rank) laminate. Indeed, the optimality condition (5.11) for the present problem takes the form

$$S_m = \max_{K_*} \left[(\nabla \lambda_a)^T K_* (\nabla u_a) + (\nabla \lambda_b)^T K_* (\nabla u_b) \right], \tag{6.4}$$

where λ_a and λ_b are conjugate variables that account for differential constraints for u_a and u_b in (6.1)–(6.2), respectively.

However, the problems for λ_a and λ_b are independent of the position of entering flux, as in (5.8), (5.9), and so are their solutions, $\lambda_a = \lambda_b = \lambda$. Therefore, the optimality condition (6.4) is similar to (5.11) applied to $u_a + u_b$ instead of u

$$S_m = \max_{K} [\nabla \lambda^T K_* \nabla (u_a + u_b)]. \tag{6.5}$$

The optimal layers bisect the angle between $\nabla \lambda$ and $\nabla (u_a + u_b)$. The volume fraction depends on the value of this angle, as above, see (5.12). The design depends only on the sum of solutions u_a and u_b , that is, the solution to the thermolens with the sum of the incoming boundary fluxes.

Symmetric heat sources. Assume now that the sources are symmetric against the *y*-axis as shown in figure 2*d*. Because of this symmetry, optimal values of I_1 and I_2 are equal, the optimal composite layout is symmetric as well, $K_*(x,y) = K_*(-x,y)$, and $\alpha = 1$. Optimal structures are laminates symmetric with respect to the *y*-axis.

7. Optimization of dynamic materials

(a) Dynamic materials

DM are defined as media that can change their material properties in space and time. This change is governed by a controller. A composite assembled from such materials becomes a dynamic composite, see [26,27,76].

Consider a transmission line characterized by density ρ and stiffness k. Assume that the wave u(x,t) propagates along the line. The equation of the motion of the wave is

$$\frac{\partial}{\partial t}\rho(x,t)\frac{\partial u}{\partial t} - \frac{\partial}{\partial x}k(x,t)\frac{\partial u}{\partial x} = 0,$$
(7.1)

where properties $\rho(x,t)$ and k(x,t) are variable in space and time. Specifically, we have two materials available (one and two), characterized each by a pair of constant properties ρ_i and k_i , i=1,2. These materials have different phase velocities $v_i(x,t) = \sqrt{k_i/\rho_i}$, i=1,2. Let $v_1 < v_2$, so that the first material is slow and the second is fast. We assume that materials have the same wave impedance $1/\sqrt{k\rho}$ in order to eliminate reflections from their interfaces and work with waves that propagate unidirectionally.

Equation (7.1) can be represented as the following system:

$$\frac{\partial u}{\partial t} = \frac{1}{\rho} \frac{\partial v}{\partial x}$$
 and $\frac{\partial v}{\partial t} = k \frac{\partial u}{\partial x}$ (7.2)

for functions u and v, which are continuous across the interfaces between the materials. Parameters ρ and k take values ρ_i , k_i in material i, i = 1, 2, periodically alternating along the line so that

$$k(x,t) = \chi(x,t)k_1 + (1-\chi(x,t))k_2$$
 and $\rho(x,t) = \chi(x,t)\rho_1 + (1-\chi(x,t))\rho_2$, (7.3)

where

$$\chi(x,t) = \chi_x(x)\chi_t(t) + (1 - \chi_x(x))(1 - \chi_t(t)) \tag{7.4}$$

and

$$\chi_{x}(x) = \begin{cases} 1 & \text{if } 0 \le x < m_{1}\delta, \\ 0 & \text{if } m_{1}\delta \le x < \delta, \end{cases} \qquad \chi_{t}(t) = \begin{cases} 1 & \text{if } 0 \le t < n_{1}\tau \\ 0 & \text{if } n_{1}\tau \le t < \tau. \end{cases}$$
 (7.5)

Here, m_1 and n_1 are spatial and temporal fractions in the double space–time period (δ, τ) . Note that besides spatial changes in the properties, the materials (or subregions occupied by these materials) also periodically switch their properties in time. These spatial and temporal property switches are represented by a doubly periodic material distribution in the (x, t)-plane shown by rectangular grid in figure 4a,b. In figure 4b, '1' and '2' indicate cells filled by materials with the slow and fast velocity, respectively, and δ and τ are spatial and temporal periods of the doubly periodic lattice. We discuss construction of this lattice below.

Temporal and spatial laminates. Let us first consider one-dimensional composites (laminates) of materials with properties changing separately in time and in space. Assume that temporal switching of material properties occurs everywhere in space; in the presence of wave, it requires work performed by an external controller. The switch is accompanied by the change of phase velocity and wave energy; dynamic materials are thermodynamically open systems. The

Figure 4. Concentration of the wave paths. (*a*) Stable (boldface line) and unstable (dashed line) limit cycles in a double periodic space—time problem corresponding to the checkerboard formed by materials with two different properties. The space coordinate is given on the horizontal axis and time is shown along the vertical axis. Stable limit cycles attract all trajectories in the corresponding basins of attraction separated by the unstable cycles representing the boundaries of the attraction basins [28]. (*b*) A stable limit cycle (a trajectory shown by the boldface line) attracts trajectories starting in the cell filled by the slow material indicated by '1', as well as in the cell with fast material denoted by '2'. (*c*) Trajectories of double-periodic system (7.2) mapped onto topologically equivalent torus [77].

temporal switch from a slow material to the fast increases the wave energy W_1 to W_2 , so that

$$\frac{W_2}{W_1} = \frac{v_2}{v_1}.$$

The opposite jump decreases the wave energy in the same proportion. The energy from the controller is absorbed by the wave in the first case and released in the second [68].

As for the controller's energy, it decreases in the first case and increases in the second due to its exchange with the wave. Two sequential temporal property switches can be depicted as a horizontal strip in the space–time diagram. A periodic array of temporal switches can be viewed as a laminate with horizontal layers, and the wave trajectory through it is a broken line with alternating slopes.

For a spatial laminate, we consider a transmission line as an array of alternating spatial intervals filled by the materials with phase velocities v_1 and v_2 . The velocity jumps at the interface between these intervals, but the energy flux remains continuous for every bunch of wave routes. The wave energy is preserved in the absence of temporal property switches. In the space–time diagram, the wave trajectory is also a broken line with alternating slopes as in the case of temporal property switches.

(b) Dynamic composites: checkerboard

Downloaded from https://royalsocietypublishing.org/ on 26 January 2024

Below, we design a structure that can focus and accumulate the wave energy. Notice that neither spatial nor temporal laminate alone can perform this task. We need the features of both types to create the required design by combining them in a doubly periodic checkerboard structure in space—time, figure 4.

Consider a doubly periodic rectangular lattice in (x,t)-plane, figure 4b. A double period is a unit square divided in four quadrants. The first and the third quadrants are occupied by the fast material (v_2) and the second and the fourth by the slow material (v_1) [27,28]. This construction results in the checkerboard material assembly in space–time. Each rectangle occupied by one material has all its faces contacting rectangles occupied by another material.

As the waves travel through this checkerboard lattice, their routes cross both types of interfaces, but these crossings differ from each other in energy performance. The energy flux stays continuous at spatial interfaces but the energy density jumps at temporal crossings, as described above. Based on that, we design a space—time geometry that accumulates and concentrates energy in travelling waves. This geometry is a checkerboard described above. It avoids energy losses

along the wave routes if all of the crossings either leave the wave energy continuous or add energy to wave. This is possible if

- (i) the waves enter the slow material from fast across a spatial interface where energy flux is preserved;
- (ii) the waves enter the fast material from slow across temporal transients when it gains energy;
- (iii) the wave routes never intersect each other and therefore avoid collision. A remarkable property of the checkerboard is that it allows for a desired performance of waves.

Design of the energy concentrators. We use four controls, the fractions m_1 and n_1 and the wave speeds v_1 , and v_2 , to construct the required structure. It has been shown in [29] that there exist ranges of these parameters that support the desirable wave routes and maintain the energy accumulation; this is visible in figure 4. Exact bounds for parameters found in [29] specify such ranges.

Below, we illustrate the results of numerical analysis described in [27–29]. In figure 4*a*, there are boldface and dashed lines. Both lines are special periodic wave routes represented by closed trajectories in space–time which are stable and unstable limit cycles. The boldface lines represent stable cycles, whereas the interrupted lines represent unstable cycles. We clearly see the difference between these cycles in figure 4. Every pair of consecutive stable cycles has an unstable cycle in between. The reason is that the trajectories (the wave routes) are attracted by stable and repelled by unstable cycles. No stable cycle enters the slow material from across the temporal interface where it would lose energy; and this is a specific feature of a checkerboard. The stable cycles are parallel because the geometry of a checkerboard in figure 4*a* is doubly periodic. The stable cycle attracting other trajectories mapped onto topologically equivalent torus [77] is shown in figure 4*c*. Figure 4*b* presents several trajectories on the space–time checkerboard with the cells formed by the regions occupied by the two materials with slow and fast velocity. The boldface line in figure 4*b* shows a stable limit cycle that attracts trajectories starting in the neighbouring cells.

Sharpening pulses. Another feature of the energy concentrating structure is that the wave routes never intersect; instead, are densely compressed and tend to the stable periodic limit circles. Accordingly, the energy is accumulated in the array of progressively sharpening pulses, figure 4*a* (limit cycles in the corresponding phase space) composed from densely compressed wave routes, see [27,28]. Remarkably, such constructions need no more than Snell's Law plus the analysis of kinematics of the wave routes that merge towards each other to be compressed in pulses as time evolves.

If the energy stored in the controlling mechanism is limited, it becomes exhausted at some instant. From that point on, the horizontal material interfaces disappear because they are no longer supported, and the checkerboard turns into a spatial laminate. The accumulated energy waves propagate through such laminate without any energy loss.

The checkerboard appearance in both linear and nonlinear cases. The previous example is related to a linear system demonstrating the motion of energy pulses through a given checkerboard material pattern in space–time. The velocity of pulses is prescribed by parameters of the pattern. A similar type of motion is observed in a nonlinear system when we deal with a spring-load (SL) unit moving on the ground in the presence of dry friction due to a constant velocity V applied to SL from outside. In this situation, periodic limit cycles also arise [78], but their spatial and temporal periods are defined by the system itself, not coming from the environment. The motion of the SL occurs in space–time in a fashion similar to the motion of pulses supported by a prescribed checkerboard. We see a similarity, not the identity of these mechanisms, and this similarity reveals that the checkerboard principle goes beyond the linear situation, now due to the loss of stability that produces self-induced oscillations.

8. Conclusion

- 1. In multi-material design, the structure is created by a distribution of the interface between domains filled with different materials. The optimal design asks for the best location of this interface. The solutions admit that the interfaces may densely cover a region between domains of pure materials, creating composite zones. The variable structure of this composite must be optimal at every point. The optimal composites are characterized by relatively simple parametrized structures that keep components of the fields in each material constant. The optimal composites can best focus and direct the currents and fluxes due to their anisotropy. Optimal design of a thermal lens demonstrates how these composite zones follow from analysis of necessary conditions of optimality.
- 2. In the case of spatio-temporal composites with properties varying in both space and time, focusing is achieved by concentrating the energy of the wave into sharp pulses. For a special range of structural parameters, the described time–space checkerboard structures can concentrate the wave energy. The wave routes are gradually concentrated in discrete paths as time tends to infinity; the paths never intersect. The paths accumulate energy and tend to a series of pulses parallel to each other.

Data accessibility. This article has no additional data.

Declaration of Al use. We have not used AI-assisted technologies in creating this article.

Authors' contributions. A.C.: conceptualization, formal analysis, investigation, writing—original draft, writing—review and editing; E.C.: conceptualization, formal analysis, investigation, writing—original draft, writing—review and editing; K.L.: conceptualization, formal analysis, investigation, writing—original draft, writing—review and editing.

All authors gave final approval for publication and agreed to be held accountable for the work performed therein.

Conflict of interest declaration. We declare we have no competing interests.

Funding. The work of A.C. was supported by the NSF DMS (grant no. 1515125). E.C. acknowledges support from the NSF (grant no. DMS-2111117).

Acknowledgements. The authors are thankful to Graeme Milton for providing additional references.

References

- 1. Milton GW, Briane M, Willis JR. 2006 On cloaking for elasticity and physical equations with a transformation invariant form. *N. J. Phys.* **8**, 248–268. (doi:10.1088/1367-2630/8/10/248)
- 2. Pendry JB, Schurig D, Smith DR. 2006 Controlling electromagnetic fields. *Science* **312**, 1780. (doi:10.1126/science.1125907)
- 3. Alu A, Engheta N. 2005 Achieving transparency with plasmonic and metamaterial coatings. *Phys. Rev. E* **95**, 016623. (doi:10.1103/PhysRevE.72.016623)
- 4. Chen H, Chan CT. 2007 Acoustic cloaking in three dimensions using acoustic metamaterials. *Appl. Phys. Lett.* **91**, 183518. (doi:10.1063/1.2803315)
- 5. Greenleaf A, Kurylev Y, Lassas M, Uhlmann G. 2007 Full-wave invisibility of active devices at all frequencies. *Commun. Math. Phys.* 275, 749–789. (doi:10.1007/s00220-007-0311-6)
- 6. Greenleaf A, Kurylev Y, Lassas M, Uhlmann G. 2012 Schrodinger's hat: electromagnetic, acoustic and quantum amplifiers via transformation optics. *Proc. Natl Acad. Sci. USA* **109**, 10169–10174. (doi:10.1073/pnas.1116864109)
- 7. Kohn RV, Shen H, Vogelius MS, Weinstein MI. 2008 Cloaking via change of variables in electric impedance tomography. *Inverse Probl.* **24**, 015016. (doi:10.1088/0266-5611/24/1/015016)
- 8. Milton GW, Nicorovici NA. 2006 On the cloaking effects associated with anomalous localised resonance. *Proc. R. Soc. A* **462**, 3027–3059. (doi:10.1098/rspa.2006.1715)
- 9. Norris A. 2008 Acoustic cloaking theory. *Proc. R. Soc. A* **464**, 2411–2434. (doi:10.1098/rspa.2008.0076)
- 10. Schurig D, Mock JJ, Justice BJ, Cummer SA, Pendry JB, Starr AF, Smith DR. 2006 Metamaterial electromagnetic cloak at microwave frequencies. *Science* **314**, 977–980. (doi:10.1126/science.1133628)
- 11. Cherkaev A, Kadic M, Milton GW, Wegener M. 2019 Pentamode materials: from underwater cloaking to cushioned sneakers. *SIAM News* **52**, 1–2.

- 12. Cherkaev A, Dzierzhanowski G. 2013 Three-phase plane composites of minimal elastic stress energy: high-porosity structures. *Int. J. Solids Struct.* **50**, 4145–4160. (doi:10.1016/j.ijsolstr.2013.08.010)
- 13. Kadic M, Milton GW, van Hecke M, Wegener M. 2019 3D metamaterials. *Nat. Rev. Phys.* **1**, 198–210. (doi:10.1038/s42254-018-0018-y)
- 14. Milton GW, Cherkaev AV. 1995 Which elasticity tensors are realizable? *J. Eng. Mater. Technol.* **117**, 483–493. (doi:10.1115/1.2804743)
- 15. Chen F, Lei DY. 2015 Experimental realization of extreme heat flux concentration with easy-to-make thermal metamaterials. *Sci. Rep.* **5**, 11552. (doi:10.1038/srep11552)
- 16. Cherkaev AV, Gibianski LV, Lurie KA. 1985 Optimum focusing of heat flux by means of a non-homogeneous heat-conducting medium. The Technical University of Denmark, Report No. 305 (Gibiansky LV, Lurie KA, Cherkaev AV. 1988 Optimal focusing of a heat flow by inhomogeneous heat-conducting media (The thermal-lens problem). J. Tech. Physics (Zhurnal Tekhnicheskoi Fiziki), 58(1), 67–74. In Russian.
- 17. Guenneau S, Amra C, Veynante D. 2012 Transformation thermodynamics: cloaking and concentrating heat flux. *Opt. Express* **20**, 8207–8218. (doi:10.1364/OE.20.008207)
- 18. Narayana S, Sato Y. 2012 Heat flux manipulation with engineered thermal materials. *Phys. Rev. Lett.* **108**, 214303. (doi:10.1103/PhysRevLett.108.214303)
- 19. Peralta I, Fachinotti V, Ciarbonetti A. 2017 Optimization-based design of a heat flux concentrator. *Sci. Rep.* 7, 40591. (doi:10.1038/srep40591)
- 20. Rahm M, Schurig D, Roberts DA, Cummer SA, Smith DR, Pendry JB. 2008 Design of electromagnetic cloaks and concentrators using form-invariant coordinate transformations of Maxwell's equations. *Photonics Nanostruct. Fundam. Appl.* **6**, 87–95. (doi:10.1016/j.photonics.2007.07.013)
- 21. Schittny R, Kadic M, Guenneau S, Wegener M. 2013 Experiments on transformation thermodynamics: molding the flow of heat. *Phys. Rev. Lett.* **110**, 195901. (doi:10.1103/PhysRevLett.110.195901)
- 22. Yago D, Cante J, Lloberas-Valls O, Oliver J. 2020 Topology optimization of thermal problems in a nonsmooth variational setting: closed-form optimality criteria. *Comput. Mech.* **66**, 259–286. (doi:10.1007/s00466-020-01850-0)
- 23. Biancalana F, Amann A, Uskov AV, O'Reilly EP. 2007 Dynamics of light propagation in spatio-temporal dielectric structures. *Phys. Rev. E* **75**, 046607. (doi:10.1103/PhysRevE.75.046607)
- 24. Blekhman II, Lurie KA. 2000 On dynamic materials. Proc. Rus. Acad. Sci. (Doklady) 37, 182–185.
- 25. Huidobro PA, Galiffi E, Guennau S, Craster RV, Pendry JB. 2019 Fresnel drag in space-time modulated metamaterials. *Proc. Natl Acad. Sci. USA* **116**, 24943–24948. (doi:10.1073/pnas.1915027116)
- 26. Lurie KA. 2009 On homogenization of activated laminates in 1D space and time. *ZAMM J. Appl. Math. Mech./Zeitschrift fur Angewandte Mathematik und Mechanik.* **89**, 333–40. (doi:10.1002/zamm.200800185)
- 27. Lurie KA. 2007 *An introduction to the mathematical theory of dynamic materials*. New York, NY: Springer.
- 28. Lurie KA, Weekes SL. 2006 Wave propagation and energy exchange in a spatio-temporal material composite with rectangular microstructure. *J. Math. Anal. Appl.* **314**, 286–310. (doi:10.1016/j.jmaa.2005.03.093)
- 29. Lurie KA, Onofrei D, Weekes SL. 2009 Mathematical analysis of the waves propagation through a rectangular material structure in space-time. *J. Math. Anal. Appl.* **355**, 180–194. (doi:10.1016/j.jmaa.2009.01.031)
- 30. Milton GW, Mattei O. 2017 Field patterns: a new mathematical object. *Proc. R. Soc. A* **473**, 20160819. (doi:10.1098/rspa.2016.0819)
- 31. Shui LQ, Yue ZF, Liu YS, Liu QC, Guo JJ. 2014 One-dimensional linear elastic waves at moving property interface. *Wave Motion* 51, 1179–1192. (doi:10.1016/j.wavemoti.2014.07.005)
- 32. Shui LQ, Yue ZF, Liu YS, Liu QC, Guo JJ, He XD. 2015 Novel composites with asymmetrical elastic wave properties. *Compos. Sci. Technol.* **113**, 19–30. (doi:10.1016/j.compscitech.2015.03.007)
- 33. Taravati S. 2018 Giant linear nonreciprocity, zero reflection, and zero band gap in equilibrated space-time-varying media. *Phys. Rev. Appl.* **9**, 064012. (doi:10.1103/PhysRevApplied.9.064012)
- 34. To HT. 2009 Homogenization of dynamic laminates. *J. Math. Anal. Appl.* **354**, 518–538. (doi:10.1016/j.jmaa.2008.12.058)

- 35. Weekes SL. 2001 Numerical computation of wave propagation in dynamic materials. *Appl. Numer. Math.* **37**, 417–440. (doi:10.1016/S0168-9274(00)00045-3)
- 36. Tsai CS. 1990 *Guided-wave acousto-optics interactions, devices, and applications*. Springer Series in Electronics and Photonics, **(SSEP, volume 23)**.
- 37. Zhou W *et al.* 2020 4D-Printed dynamic materials in biomedical applications: chemistry, challenges, and their future perspectives in the clinical sector. *J. Med. Chem.* **63**, 8003–8024. (doi:10.1021/acs.jmedchem.9b02115)
- 38. Pontryagin LS, Boltyanskii VG, Gamkrelidze RV, Mischenko EF. 1962 *The mathematical theory of optimal processes*. New York, NY: John Wiley and Sons, Inc.
- 39. Rozonoer LI. 1959 Pontryagin's maximum principle in the theory of optimal systems. I, II, III. *Automat. Remote Control* **20**, 11–12.
- 40. Gamkrelidze RV. 1978 Principles of optimal control theory. Boston, MA: Springer.
- 41. Kohn RV, Strang G. 1986 Optimal design and relaxation of variational problems, I, II, III. *Commun. Pure Appl. Math.* **39**, 113–137, 139–182, 353–377. (doi:10.1002/cpa.3160390107)
- 42. Murat F, Tartar L. 1985 Calculus of variations and homogenization. Les Methodes de l'Homogeneisation: Theorie et Applications en Physique, Eyrolles, 319–369. English translation in: Topics in the Mathematical Modelling of Composite Materials. Cherkaev A, Kohn RV, eds, Birkhauser, Boston, 1997, 139–173.
- 43. Murat F, Tartar L. 1975 *On the control of coefficients in partial differential equations*. Lecture Notes in Economics and Mathematical Systems, **107**. Springer, pp. 420–426. English translation in: Topics in the Mathematical Modelling of Composite Materials. Cherkaev A, Kohn RV, eds, Birkhauser, Boston, 1997, 1–8.
- 44. Tartar L. 1985 Estimation fines des coefficients homogeneises. Ennio de Giorgi Colloquium, Kree P (ed), Pitman Research Notes in Math. 125, 168–187. English translation in: Topics in the Mathematical Modelling of Composite Materials. Cherkaev A, Kohn RV (eds), Birkhauser, Boston, 1997, 9–20.
- 45. Bendsoe MP, Sigmund O. 2003 Topology optimization: theory, methods, and applications. Springer.
- 46. Sigmund O. 1994 Materials with prescribed constitutive parameters: an inverse homogenization problem. *Int. J. Solids Struct.* **31**, 2313–2329. (doi:10.1016/0020-7683(94)90154-6)
- 47. Sigmund O. 1995 Tailoring materials with prescribed elastic properties. *Mech. Mater.* **20**, 351–368. (doi:10.1016/0167-6636(94)00069-7)
- 48. Allaire G. 2002 Shape optimization by the homogenization method. Springer.
- 49. Francfort GA, Milton GW. 1994 Sets of conductivity and elasticity tensors stable under lamination. *Comm. Pure Appl. Math.* 47, 257–279. (doi:10.1002/cpa.3160470302)
- 50. Milton GW. 1986 Modelling the properties of composites by laminates. In *Homogenization and effective moduli of materials and media* (eds JL Ericksen, D Kinderlehrer, RV Kohn, JL Lions), pp. 150–174. New York, NY: Springer.
- 51. Milton GW. 2002 Theory of composites. Cambridge, UK: Cambridge University Press.
- 52. Cherkaev A. 2000 Variational methods for structural optimization. Springer.
- 53. Lurie KA. 2013 Applied optimal control theory of distributed systems. Springer Science & Business Media.
- 54. Lurie KA, Cherkaev AV, Fedorov AV. 1982 Regularization of optimal design problems for bars and plates. *J. Optim. Theory Appl.* 37, 499–522. (doi:10.1007/BF00934953)
- 55. Cherkaev A. 1994 Relaxation of problems of optimal structural design. *Int. J. Solids Struct.* **31**, 2251–2280. (doi:10.1016/0020-7683(94)90209-7)
- 56. Cherkaev A, Gibiansky L. 1992 The exact coupled bounds for effective tensors of electrical and magnetic properties of two-component, two-dimensional composites. *Proc. R. Soc. Edin. A*, **122**, 93–125. (doi:10.1017/S0308210500020990)
- 57. Cherkaev A, Gibiansky L. 1993 Coupled estimates for the bulk and shear moluli of a two-dimensional isotropic elastic composite. *J. Mech. Phys. Solids* **41**, 937–980. (doi:10.1016/0022-5096(93)90006-2)
- 58. Lurie KA, Cherkaev AV. 1984 Exact estimates of conductivity of composites formed by two isotropically conducting media taken in prescribed proportion. *Proc. R. Soc. Edin. A* **99**, 71–87. (doi:10.1017/S030821050002597X)
- 59. Lurie KA, Cherkaev AV, Fedorov AV. 1984 On the existence of solutions to some problems of optimal design for bars and plates. *J. Optim. Theory Appl.* **42**, 247–281. (doi:10.1007/BF00934299)

- 60. Braides A. 2002 Gamma-convergence for beginners. Oxford, UK: Oxford University Press.
- 61. Jikov VV, Kozlov SM, Oleinik OA. 1994 Homogenization of differential operators and integral functionals. Springer.
- 62. Papanicolaou G, Bensoussan A, Lions JL. 1978 *Asymptotic analysis for periodic structures*. Amsterdam, the Netherlands: Elsevier.
- 63. Cherkaev A, Cherkaev E. 1999 Optimal design for uncertain loading conditions. In *Homogenization* (eds V Berdichevsky, V Jikov, G Papanicolaou), pp. 193–213. World Scientific.
- 64. Cherkaev E, Cherkaev A. 2003 Principal compliance and robust optimal design. *J. Elast.* **72**, 71–98. (doi:10.1023/B:ELAS.0000018772.09023.6c)
- 65. Cherkaev E, Cherkaev A. 2008 Minimax optimization problem of structural design. *Int. J. Comput. Struct.* **86**, 1426–1435. (doi:10.1016/j.compstruc.2007.05.026)
- 66. Brittain K, Silva M, Tortorelli DA. 2012 Minmax topology optimization. *Struct. Multidisc. Optim.* 45, 657–668. (doi:10.1007/s00158-011-0715-y)
- 67. de Gournay F, Allaire G, Jouve F. 2008 Shape and topology optimization of the robust compliance via the level set method. *ESAIM: Control, Optim. Calc. Variat.* **14**, 43–70. (doi:10.1051/cocv:2007048)
- 68. Morgenthaler FR. 1958 Velocity modulation of electromagnetic waves. *IRE Trans. Microwave Theory Tech.* **6**, 167–172. (doi:10.1109/TMTT.1958.1124533)
- 69. Lurie KA. 1997 Effective properties of smart elastic laminates and the screening phenomenon. *Int. J. Solids Struct.* **34**, 1633–1643. (doi:10.1016/S0020-7683(96)00105-9)
- 70. Eshelby JD. 1959 The elastic field outside an ellipsoidal inclusion. *Proc. R. Soc. Lond. A* **252**, 561–569. (doi:10.1098/rspa.1959.0173)
- 71. Lurie KA, Cherkaev AV. 1986 Exact estimates of the conductivity of a binary mixture of isotropic materials. *Proc. R. Soc. Edin. A* **104**, 21–38. (doi:10.1017/S0308210500019041)
- 72. Hashin Z, Shtrikman S. 1963 A variational approach to the elastic behavior of multiphase minerals. *J. Mech. Phys. Solids* **11**, 127–140. (doi:10.1016/0022-5096(63)90060-7)
- 73. Benveniste Y, Milton GW. 2003 New exact results for the effective electric, elastic, piezoelectric and other properties of composite ellipsoid assemblages. *J. Mech. Phys. Solids* **51**, 1773–1813. (doi:10.1016/S0022-5096(03)00074-7)
- 74. Cherkaev A. 2012 Optimal three-material wheel assemblage of conducting and elastic composites. *Int. J. Eng. Sci.* **59**, 27–39. (doi:10.1016/j.ijengsci.2012.03.007)
- 75. Cherkaev A, Cherkaev E. 1999 Structural optimization and biological 'designs'. In *IUTAM Symp. on Synthesis in Bio Solid Mechanics* (eds P Pedersen, M Bendsoe), pp. 247–264. Dordrecht, the Netherlands: Springer Science and Business Media.
- 76. Blekhman II. 2007 On vibratory dynamic materials and composites. *Proc. Rus. Acad. Sci.* (*Doklady*) **52**, 335–338. (doi:10.1134/S1028335807060110)
- 77. Sanguinet WC, Lurie KA. 2013 Propagation of dilatation and shear waves through a dynamic checkerboard material geometry in 1D space + time. *ZAMM* **93**, 937–943. (doi:10.1002/zamm.201200249)
- 78. Panovko YG. 1980 An introduction to the theory of mechanical vibrations. Moscow: Nauka (in Russian).